

# Analysis and Optimization of Dynamically Loaded Reinforced Plates by the Coupled Boundary and Finite Element Method

P. Fedelinski<sup>1</sup> and R. Gorski<sup>1</sup>

**Abstract:** The aim of the present work is to analyze and optimize plates in plane strain or stress with stiffeners subjected to dynamic loads. The reinforced structures are analyzed using the coupled boundary and finite element method. The plates are modeled using the dual reciprocity boundary element method (DR-BEM) and the stiffeners using the finite element method (FEM). The matrix equations of motion are formulated for the plate and stiffeners. The equations are coupled using conditions of compatibility of displacements and equilibrium of tractions along the interfaces between the plate and stiffeners. The final set of equations of motion is solved step-by-step using the Houbolt direct integration method. The direct solutions are displacements and tractions for boundary and interface nodes in each time step. The aim of optimization is to find the optimal lengths and locations of stiffeners. The objective functions, which characterize strength and stiffness, depend on displacements or tractions. The optimization problem is solved using an evolutionary method. The results of the dynamic analysis by the proposed method are compared with the solutions computed by the professional finite element code, showing a very good agreement. As the result of optimization, an improvement of dynamic response is obtained, in comparison with an initial design.

**keyword:** Dynamics, Optimization, Plate, Stiffener, Boundary element method, Finite element method, Evolutionary method.

## 1 Introduction

Structures are reinforced by stiffeners in order to increase strength, stiffness and stability. The stiffened structures are frequently subjected to dynamic loads, and the knowledge of their transient dynamic response has a practical significance. Optimal choice of a number of stiffeners, their properties and locations in the structure decides about the effectiveness of the reinforcement.

An analysis of structures with arbitrary geometry, material properties and boundary conditions requires numerical methods. One of the versatile methods, which is intensively developed in dynamics of solids, is the boundary element method (BEM) [Dominguez (1993)]. The method has been used in static and dynamic analysis of structures with stiffeners. Salgado and Aliabadi (1996,1998,1999) presented the analysis of statically loaded stiffened panels with cracks. The dual BEM was used for sheets with cracks and analytical equations for stiffeners. Growth of single and multiple cracks was considered. Coda, Venturini (1999), Coda, Venturini and Aliabadi (1999) showed the coupling of 3D bodies, modeled by the BEM, with shells, plates and frames, analyzed by the FEM. The proposed method is particularly suitable to analysis of soil-structure interactions. Coda (2001) presented a static and dynamic non-linear analysis of reinforced 2D structures. The plates were modeled using the BEM and reinforced by non-linear trusses modeled by the FEM. Numerical solutions for a concrete reinforced beam were compared with experimental results. Leite, Coda and Venturini (2003) presented a particular approach for 2D reinforced structures, in which bars were represented by very thin sub-regions. In this method, tractions along the interfaces were eliminated from equations. Leite and Venturini (2005) presented an alternative formulation, in which displacements at interfaces were eliminated. Botta and Venturini (2005) used the boundary-finite element combination to analyze 2D elastostatic solids reinforced by fibers. The debonding effects between the matrix and fibers were considered. Forth and Staroselsky (2005) applied the hybrid finite and boundary element approach to model a 3D crack propagating through a thin multilayered coating. The method was implemented to design an aircraft engine structural health monitoring system.

In this work, a static and dynamic analysis and optimization of plates with stiffeners is presented. The plates are modeled by the BEM and the stiffeners by the FEM. The optimization problem is solved by the evolutionary

---

<sup>1</sup> Silesian University of Technology, Gliwice, Poland

method. The preliminary results of optimization were presented by Gorski and Fedelinski (2004,2005). In those works, the stiffeners were attached at boundaries of the plates. In the present work, the reinforcement is in the interior of 2D structures.

## 2 Boundary integral equations for the plate

Let us consider a two-dimensional, homogenous, isotropic and linear elastic body with the boundary  $\Gamma^1$  occupying the domain  $\Omega^1$ . The body is subjected to dynamic boundary tractions and body forces distributed in the domain  $\Omega^2$ , as shown in Fig.1.

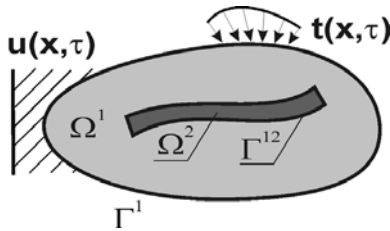


Figure 1 : A plate reinforced by a stiffener

The following boundary conditions:

$$\begin{aligned} u_i(x, \tau) &= \bar{u}_i(x, \tau) \text{ on } \Gamma^u, \text{ and} \\ t_i(x, \tau) &= \sigma_{ij}(x, \tau)n_j = \bar{t}_i(x, \tau) \text{ on } \Gamma^t, \end{aligned} \quad (1)$$

and initial conditions:

$$u_i(x, 0) = u_i^o(x) \text{ and } \dot{u}_i(x, 0) = v_i^o(x) \text{ in } \Omega^1, \quad (2)$$

are imposed, where:  $u_i$  is the component of displacement,  $t_i$  is the component of traction,  $\bar{u}_i$  and  $\bar{t}_i$  denote the prescribed boundary conditions,  $\sigma_{ij}$  is the stress tensor,  $n_j$  is the component of the outward normal versor at the boundary,  $\Gamma^u$  and  $\Gamma^t$  are parts of the boundary  $\Gamma^1$  ( $\Gamma^u \cup \Gamma^t = \Gamma^1$ ),  $u_i^o$  and  $v_i^o$  are the prescribed initial conditions,  $x$  are coordinates of a point,  $\tau$  is a time; repeated indices denote the summation convention and overdots indicate time derivatives; the indices for two-dimensional problems are  $i, j = 1, 2$ . Zero initial conditions are considered in this work.

The relation between the mechanical fields can be ex-

pressed by the integral equation [Dominguez (1993)]

$$\begin{aligned} c_{ij}(x')u_j(x', \tau) &= \int_{\Gamma^1} U_{ij}(x', x)t_j(x, \tau)d\Gamma(x) \\ &- \int_{\Gamma^1} T_{ij}(x', x)u_j(x, \tau)d\Gamma(x) \\ &- \rho \int_{\Omega^1} U_{ij}(x', X)\ddot{u}_j(X, \tau)d\Omega(X) \\ &+ \rho \int_{\Omega^2} U_{ij}(x', X)b_j(X)d\Omega(X) \end{aligned} \quad (3)$$

where:  $c_{ij}$  is a constant, which depends on the position of the point,  $\rho$  is a mass density,  $b_j$  is a body force,  $U_{ij}$  and  $T_{ij}$  are fundamental solutions of elastostatics,  $x'$  is a collocation point,  $x$  is a boundary point and  $X$  is a domain point.

The inertial domain integral in Eq.3 is transformed into the boundary integrals using the dual reciprocity method (DRM) proposed by Brebbia and Nardini (1983) [see also Dominguez (1993)]. In this method, it is assumed that the accelerations are interpolated using the equation

$$\ddot{u}_i(X, \tau) = \ddot{\alpha}_i^n(\tau)f^n(x^*, X) \quad (4)$$

where  $\ddot{\alpha}_i^n$  is a time-dependent function and  $f^n$  is a coordinate function. In the present work the following function is chosen

$$f^n(x^*, X) = r + C \quad (5)$$

where  $r$  is the distance between a defining point  $x^*$  and the point  $X$ , and  $C$  is a constant. The defining point can be a boundary or a domain point.

After the transformation, the inertial domain term in Eq.3 has the form

$$\begin{aligned} &\rho \int_{\Omega^1} U_{ij}(x', X)\ddot{u}_j(X, \tau)d\Omega(X) \\ &= \rho[-c_{ij}(x')\hat{u}_{jl}^n(x^*, x')] \\ &+ \int_{\Gamma^1} U_{ij}(x', x)\hat{t}_{jl}^n(x^*, x)d\Gamma(x) \\ &- \int_{\Gamma^1} T_{ij}(x', x)\hat{u}_{jl}^n(x^*, x)d\Gamma(x)]\ddot{\alpha}_i^n(\tau) \end{aligned} \quad (6)$$

where:  $\hat{u}_{jl}^n$  and  $\hat{t}_{jl}^n$  are fictitious displacements and tractions [Dominguez (1993)], respectively, corresponding to the fictitious body force  $f^n$  defined by Eq.5.

If the plate is reinforced by a beam, the deformed stiffener acts on the plate along the line of attachment. In this case, the body forces  $b_j$  are tractions  $t_j$ , which are distributed along the interface line  $\Gamma^{12}$  (see Fig.1). Therefore, the integral Eq.3 has the form

$$\begin{aligned}
 c_{ij}(x')u_j(x', \tau) &= \int_{\Gamma^1} U_{ij}(x', x)t_j(x, \tau)d\Gamma(x) \\
 &- \int_{\Gamma^1} T_{ij}(x', x)u_j(x, \tau)d\Gamma(x) \\
 &+ \rho[c_{ij}(x')\hat{u}_{jl}^n(x^*, x')] \\
 &- \int_{\Gamma^1} U_{ij}(x', x)\hat{t}_{jl}^n(x^*, x)d\Gamma(x) \\
 &+ \int_{\Gamma^1} T_{ij}(x', x)\hat{u}_{jl}^n(x^*, x)d\Gamma(x)]\ddot{\alpha}_i^n(\tau) \\
 &+ \int_{\Gamma^{12}} U_{ij}(x', X)t_j(X)d\Gamma(X)
 \end{aligned} \tag{7}$$

It can be noticed, that the equation of motion of the reinforced plate is expressed in the boundary integral form.

### 3 Matrix equation for the reinforced plate

In the literature, several methods of combining of the BEM with FEM are presented. One of these approaches, which is used in the present paper, consists in treating the finite element region as an equivalent boundary element domain. Matrix equations of motion for the plate, the stiffener and the coupled equations are given in this section.

#### 3.1 Matrix equation for the plate (BEM)

In order to obtain the numerical solution for the plate, the boundary and the interface where the stiffener is attached, are divided into boundary elements. In the proposed method, quadratic 3-node elements are used. The boundary integral equations are applied for collocation points, which are nodes along the boundary and interface. The variations of boundary coordinates, displacements, tractions and interface tractions are interpolated using quadratic shape functions. Additional domain nodes (the so called internal points), which improve interpolation of accelerations, are not used in numerical examples. The set of resulting algebraic equations can be written in a

matrix form [Dominguez (1993)]

$$\begin{aligned}
 &[ \mathbf{M}^1 \quad \mathbf{M}^{12} ] \begin{Bmatrix} \ddot{\mathbf{u}}^1 \\ \ddot{\mathbf{u}}^{12} \end{Bmatrix} + [ \mathbf{H}^1 \quad \mathbf{H}^{12} ] \begin{Bmatrix} \mathbf{u}^1 \\ \mathbf{u}^{12} \end{Bmatrix} \\
 &= [ \mathbf{G}^1 \quad \mathbf{G}^{12} ] \begin{Bmatrix} \mathbf{t}^1 \\ \mathbf{t}^{12} \end{Bmatrix}
 \end{aligned} \tag{8}$$

where:  $\mathbf{M}$  is the mass matrix,  $\mathbf{H}$  and  $\mathbf{G}$  are the BEM coefficient matrices,  $\mathbf{u}$  and  $\ddot{\mathbf{u}}$  are displacement and acceleration vectors, respectively, and  $\mathbf{t}$  is a vector of tractions applied at the boundary or interface. The superscripts denote the matrices, which correspond to the boundary or interface.

#### 3.2 Matrix equation for the stiffener (FEM)

The stiffener is divided into 2-node straight finite beam elements (3 degrees of freedom in a node). After the discretization and interpolation of displacements, the equation of motion for the stiffener can be written in a matrix form [Zienkiewicz and Taylor (2000)]

$$\mathbf{M}^{21}\ddot{\mathbf{u}}^{21} + \mathbf{K}^{21}\mathbf{u}^{21} = \mathbf{T}^{21}\mathbf{t}^{21} \tag{9}$$

where:  $\mathbf{K}$  is the FEM stiffness matrix,  $\mathbf{T}$  is the matrix, which expresses the relationship between the FE nodal forces and the BE tractions. The matrix  $\mathbf{T}$  for a single finite element of length  $l$  has the form [Leite, Coda and Venturini (2003)]

$$\mathbf{T} = \begin{bmatrix} \frac{l}{3} & 0 & 0 & \frac{l}{6} & 0 & 0 \\ 0 & \frac{7l}{20} & -\frac{1}{2} & 0 & \frac{3l}{20} & -\frac{1}{2} \\ 0 & \frac{l^2}{20} & \frac{l}{12} & 0 & \frac{l^2}{30} & -\frac{l}{12} \\ \frac{l}{6} & 0 & 0 & \frac{l}{3} & 0 & 0 \\ 0 & \frac{3l}{20} & \frac{1}{2} & 0 & \frac{7l}{20} & \frac{1}{2} \\ 0 & -\frac{l^2}{30} & -\frac{l}{12} & 0 & -\frac{l^2}{20} & \frac{l}{12} \end{bmatrix} \tag{10}$$

#### 3.3 Matrix equation for the reinforced plate (coupled BEM/FEM)

If the stiffener is bonded to the plate, and the structure is subjected to boundary conditions, the interaction forces between the plate and the stiffener act along the connection line  $\Gamma^{12}$ . The displacement compatibility conditions and the traction equilibrium conditions over the interface  $\Gamma^{12}$  are

$$\mathbf{u}^{12} = \mathbf{u}^{21}; \mathbf{t}^{12} = -\mathbf{t}^{21} \tag{11}$$

If the above conditions are taken into account in Eqs 8 and 9, then the following system of equations for the whole structure is obtained

$$\begin{bmatrix} M^1 & M^{12} \\ 0 & M^{21} \end{bmatrix} \begin{Bmatrix} \ddot{u}^1 \\ \ddot{u}^{12} \end{Bmatrix} + \begin{bmatrix} H^1 & H^{12} & -G^{12} \\ 0 & K^{21} & T^{21} \end{bmatrix} \begin{Bmatrix} u^1 \\ u^{12} \\ t^{12} \end{Bmatrix} = \begin{bmatrix} G^1 \\ 0 \end{bmatrix} \{t^1\} \quad (12)$$

The above system of equations is rearranged according to the boundary conditions and solved step-by-step by the Houbolt direct integration method giving the unknown displacements and tractions on the external boundary and at the interface in each time step. The method can be used for the static analysis by assuming that the accelerations of all nodes are equal to zero. In a similar way, the method can be implemented for more stiffeners.

#### 4 Evolutionary method of optimization

The aim of optimization is to find the optimal lengths and locations of stiffeners. The design variables are coordinates of characteristic points of stiffeners. The constraints are imposed on these coordinates. The objective functions, which characterize strength or stiffness, depend on displacements or tractions.

The optimization problem is solved using an evolutionary algorithm (EA) [Goldberg (1989), Michalewicz (1996)]. The algorithm imitates evolutionary processes in nature. Contrary to the gradient methods of optimization, which require sensitivities of objective functions, the evolutionary methods can be simply implemented because they need only the values of objective functions. The probability of obtaining of the global optimal solution is very high, but the methods are very time consuming.

The evolutionary algorithm used in the paper is a modified simple genetic algorithm which uses modified genetic operators and the floating point representation. The computation starts using the initial population of chromosomes randomly generated from the feasible solution domain. Each chromosome, which consists of genes (design variables), is responsible for exactly one potential solution. An objective function plays the role of a fitness function. Chromosomes are estimated using a fit-

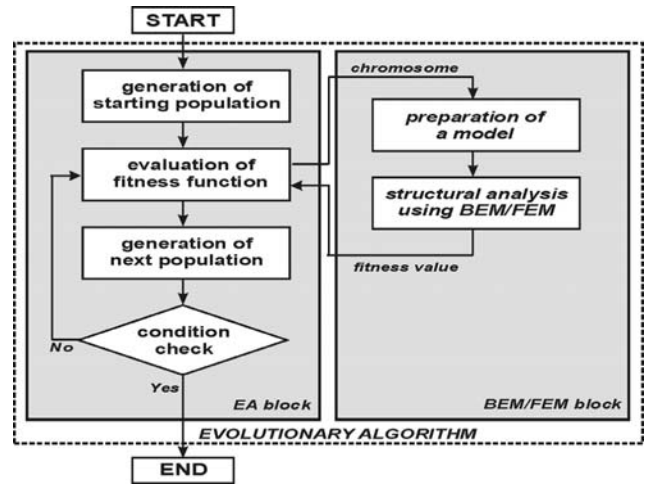


Figure 2 : An evolutionary algorithm

ness function and some of them are selected for the next generation. Meanwhile, the genetic operators and the selection are applied. On each gene appropriate constraints are imposed. This procedure is repeated until the optimal solution is reached. The solution of the problem is given by the best chromosome of all generations. Genes of this chromosome define the optimal geometry of a structure.

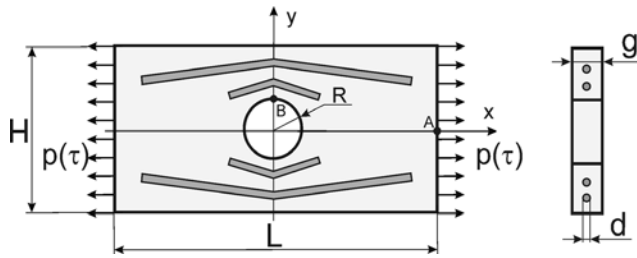
The evolutionary program consisting of two main blocks, shown in Fig.2, has been developed. To evaluate a fitness function for each chromosome, first the parameters which specify geometry of a structure are randomly generated. Then the BEM/FEM model is prepared. After that, the BEM/FEM analysis is performed and displacements and tractions on the external boundary and the interfaces are obtained. Finally, a fitness function is evaluated using the boundary displacements or tractions.

#### 5 Numerical examples

##### 5.1 Reinforced plate with a hole

The aim of the example is analysis and optimization of a rectangular plate with a hole reinforced by 4 beams of circular cross-section and statically or dynamically loaded, as shown in Fig.3.

The plate is stretched by the uniformly distributed load applied at the left and right edge. For the dynamic case, the load  $p(\tau)$  is defined by a Heaviside impulse. The value of the load is  $p=10MPa$ . The length and the height of the structure and the hole radius are respectively  $L=10cm$ ,  $H=5cm$  and  $R=1cm$ . The thickness of the plate


**Figure 3** : Reinforced plate with a hole

is  $g=1\text{ cm}$ , the diameter of each beam is  $d=0.3\text{ cm}$ . The materials of the plate ( $p$ ) in plane stress and the stiffeners ( $s$ ) are epoxy and steel, respectively. The materials of the plate and the beams are homogeneous, isotropic and linear elastic. The values of mechanical properties are as follows: modulus of elasticity  $E_p=4.5\text{ GPa}$  and  $E_s=210\text{ GPa}$ , Poisson's ratio  $\nu_p=0.37$  and  $\nu_s=0.3$ , density  $\rho_p=1160\text{ kg/m}^3$  and  $\rho_s=7860\text{ kg/m}^3$ .

The aim of optimization is to find the location of the reinforcement in the interior of the plate. The following objective functions  $J$  for statics and dynamics are considered:

minimization of the stress concentration factor  $K$  at the point B (see Fig.3)

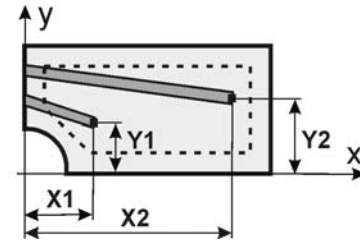
$$J = K = \frac{\sigma_{\max}^B(\tau)}{\sigma_{nom}} \quad (13)$$

minimization of the average horizontal displacement along the loaded edge in the analyzed time (maximization of stiffness)

$$J = u_{aver} = \frac{1}{N} \sum_{n=1}^N \frac{1}{M} \sum_{m=1}^M u_x^{nm} \quad (14)$$

where  $\sigma_{\max}^B(\tau)$  is the static or maximal dynamic normal stress at the point B,  $\sigma_{nom}$  is a nominal static stress at the weakened cross-section, defined as a ratio of the applied load to the area of this cross-section,  $u_x^{nm}$  is a horizontal displacement at a node  $m$  on the loaded edge and at the time step  $n$ ,  $M$  is a number of all nodes at the half of the loaded edge,  $N$  is a number of time steps.

It is assumed that during optimization the reinforcement is symmetrical with respect to two symmetry axes thus only the quarter of the structure (the upper right part) with two beams and the appropriate boundary conditions at the symmetry axes is modeled.


**Figure 4** : Design variables and constraints

The objective functions given by (13) and (14) are minimized with respect to design variables ( $X_i, Y_i, i=1,2$ ), defining the coordinates of the end of the  $i$ -th beam (see Fig.4).

The coordinates of the beginning of 2 beams at the symmetry line are fixed: the  $x$  coordinates are equal to  $0\text{ cm}$  and the  $y$  coordinates are equal to  $1.5\text{ cm}$  and  $2\text{ cm}$  for the beam near the hole and the outer boundary, respectively. The number of design variables is 4 on which the constraints are imposed. The ends of the beams can move inside the area of the dashed-line pentagon, shown in Fig.4. The connection or intersection of beams is not admissible and the distance between the beams and the boundary can not be lower than  $0.5\text{ cm}$ .

The total number of boundary and finite elements in the BEM/FEM analysis is 92 and 64, respectively (each beam is discretized into 32 finite elements). The total number of quadrilateral plate and beam finite elements in the FEM analysis is 413 and 64, respectively. The time of analysis is  $300\text{ }\mu\text{s}$  and the time step  $\Delta t=3\text{ }\mu\text{s}$ . The number of chromosomes in the population is 10 and the number of generations of the EA is 200.

### 5.1.1 Dynamic analysis

The accuracy of the developed method is investigated. The dynamic analysis is performed for the plate before optimization, called the reference plate (design variables for this plate are given in Tab.1 and Tab.2).

The dynamic horizontal displacement at the point A (see Fig.3), obtained by the present coupled BEM/FEM and by the professional FEM Nastran code, is presented in Fig.5. The agreement of the results is good.

### 5.1.2 Minimization of a stress concentration factor $K$

The results of optimization obtained by the evolutionary algorithm for the static and dynamic problem are pre-

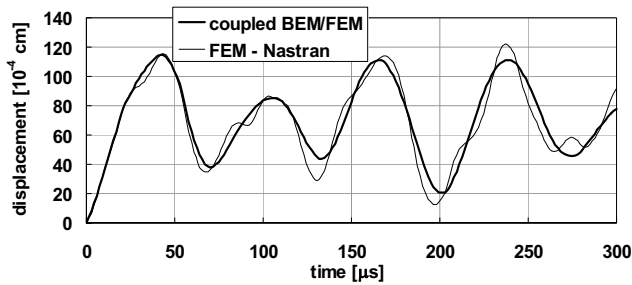


Figure 5 : Displacement at the point A

Table 1 : Values of design variables,  $J$  and  $R$

Loading	Plate	Design variables [cm]				$J$	$R$ [%]
		X1	X2	Y1	Y2		
static	non-stiffened	-				2.23	-
	reference	4.50	4.50	1.50	2.00	0.59	73.5
	optimal	2.81	4.50	1.50	2.00	0.57	74.4
dynamic	non-stiffened	-				5.16	-
	reference	4.50	4.50	1.50	2.00	1.27	75.4
	optimal	1.65	4.28	1.50	2.00	1.20	76.7

sented. The criterion of optimization is minimization of the stress concentration factor  $K$  at the point B given by (13). The values of design variables for the optimal solutions, the values of the stress concentration factors ( $SCF$ ) and their reduction  $R=(J_o - J)/J_o \cdot 100\%$  (where:  $J_o$  is the  $SCF$  for the plate without stiffeners and  $J$  is the  $SCF$  for the reference or the optimal plate), are presented in Tab.1.

It can be observed that the reduction  $R$  for the reference plate and the optimal designs is significant in comparison with the plate without the reinforcement. The values of the  $SCF$  are similar for the reference and the optimal plates, as for the static as for the dynamic load. It is due to similar location and the length of the reinforcement in the interior of the plate.

The optimal structures for statics and dynamics are shown in Fig.6a and Fig.6b. For the optimal designs the beams are parallel to the direction of the applied load.

### 5.1.3 Maximization of stiffness

The results of optimization obtained by the evolutionary algorithm, when the criterion of optimization is mini-

Table 2 : Values of design variables,  $J$  and  $R$

Loading	Plate	Design variables [cm]				$J$ [ $10^{-4}cm$ ]	$R$ [%]
		X1	X2	Y1	Y2		
static	non-stiffened	-				133	-
	reference	4.50	4.50	1.50	2.00	53	60.2
	optimal	4.50	4.50	0.89	2.00	50	62.4
dynamic	non-stiffened	-				126	-
	reference	4.50	4.50	1.50	2.00	53	57.9
	optimal	4.50	4.50	0.92	2.00	51	59.5

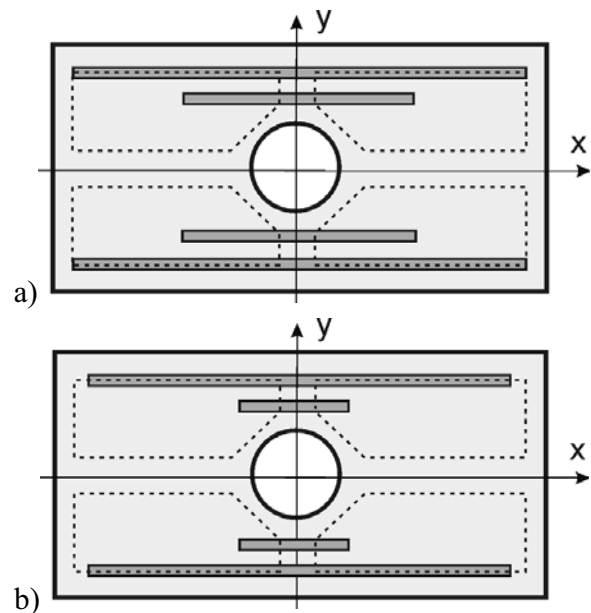


Figure 6 : Optimal structures: a) statics, b) dynamics

mization of the average horizontal displacement ( $u_{aver}$ ) along the loaded edge given by (14), are presented. The values of design variables for the optimal designs, the values of  $J$  and its reduction  $R=(J_o - J)/J_o \cdot 100\%$  (where:  $J_o$  is the  $u_{aver}$  for the plate without stiffeners and  $J$  is the  $u_{aver}$  for the reference or the optimal plate), are shown in Tab.2.

As in the previous example, the reduction  $R$  for the reference plate and the optimal designs is significant in comparison with the plate without reinforcement. Due to similar location and the length of the stiffeners for the reference and the optimal plate, the values of the average displacements are similar for the static and the dynamic

**Table 3 :** Constraints on design variables

Variable	Constraints [cm]
X1, X3	0.50÷4.75
X2, X4	5.25÷9.50
Y1, Y3	0.50÷2.25
Y2, Y4	2.75÷4.50

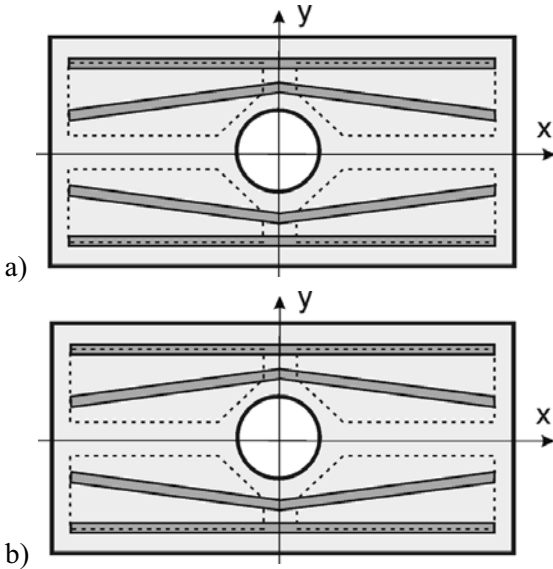


**Figure 7 :** Optimal structures: a) statics, b) dynamics

load.

The optimal structures for statics and dynamics are shown in Fig.7a and Fig.7b.

**5.2 Reinforced cantilever plate**

The aim of the example is analysis and optimization of a rectangular cantilever plate reinforced by a frame structure and statically or dynamically loaded, as shown in Fig.8. The frame is composed of 4 straight beams of square cross-section ( $2a \times b$ ). The length and the height of the plate are  $L=10\text{ cm}$  and  $H=5\text{ cm}$ , respectively. The thickness of the plate is  $g=0.25\text{ cm}$ , the dimensions of cross-section of beams are  $2a=0.5\text{ cm}$  and  $b=0.5\text{ cm}$ . The plate is fixed at its left edge and the uniformly distributed load is applied at the upper edge. For the dynamic problem, the plate is subjected to the sinusoidal load  $p(\tau)=p_o \sin(2\pi\tau/T)$ . The amplitude of the load is  $p_o=10\text{ MPa}$  and the period of time is  $T=20\pi\ \mu\text{s}$ . The material of the plate in plane stress and the frame is aluminum

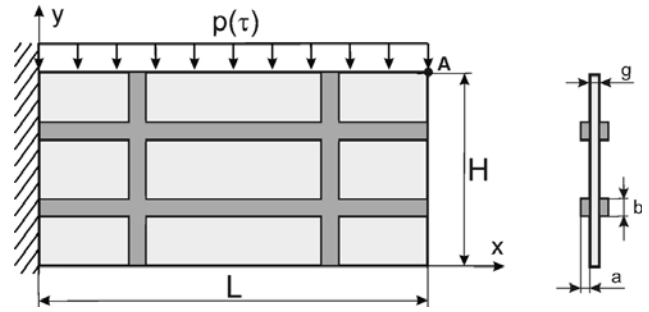


**Figure 8 :** Reinforced cantilever plate

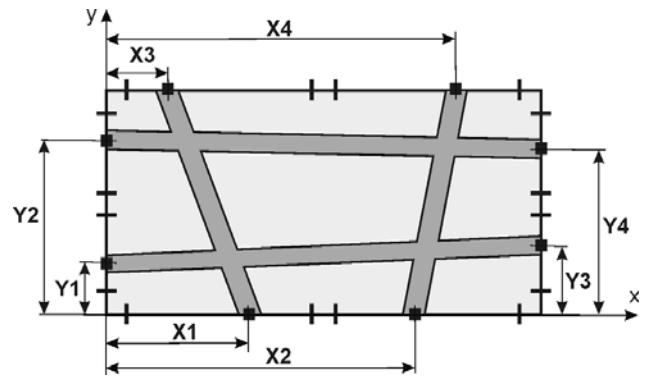


**Figure 9 :** Design variables and constraints

for which the values of mechanical properties are: modulus of elasticity  $E=70\text{ GPa}$ , Poisson’s ratio  $\nu=0.34$  and density  $\rho=2700\text{ kg/m}^3$ . The material is homogeneous, isotropic and linear elastic.

The aim of optimization is to find the location of the reinforcement (the shape of the frame) in order to maximize stiffness of the plate. The following objective function  $J$  is considered:

minimization of the vertical displacement at the point A (see Fig.8)

$$J = \max |u^A(\tau)| \tag{15}$$

where  $u^A(\tau)$  is the static or dynamic vertical displacement at the considered point A.

The number of design variables defining the shape of the frame is 8 (see Fig.9). They are the coordinates of the ends of all straight beams ( $X_i, Y_i, i=1,2,3,4$ ). The position of each beam is defined by 2 design variables on which the constraints are imposed. The ends of beams can move along the edges of the plate within the constraints, as shown in Fig.9. The constraints on the  $X_1$ ,

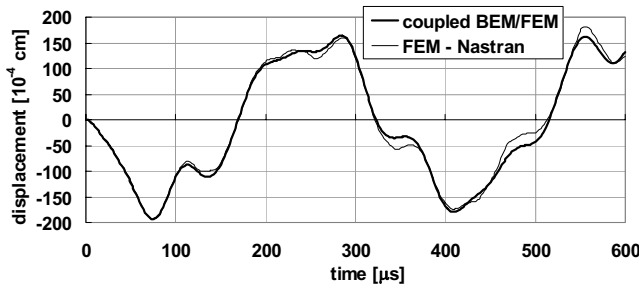


Figure 10 : Displacement at the point A

Table 4 : Values of design variables,  $J$  and  $R$

Loading	Plate	Design variables [cm]				$J$ [ $10^4$ cm]	$R$ [%]
		X1	X2	X3	X4		
		Y1	Y2	Y3	Y4		
static	non-stiffened	-				885	-
	reference	2.50 1.50	7.50 3.50	2.50 1.50	7.50 3.50	793	10.3
	optimal	4.75 0.50	7.05 4.50	0.50 1.10	9.50 4.50	487	45.0
dynamic	non-stiffened	-				430	-
	reference	2.50 1.50	7.50 3.50	2.50 1.50	7.50 3.50	193	55.2
	optimal	2.71 0.50	9.50 4.50	4.75 2.25	9.50 4.50	148	65.6

$X_2$ ,  $X_3$  and  $X_4$  variables and  $Y_1$ ,  $Y_2$ ,  $Y_3$  and  $Y_4$  variables are given in Tab.3.

The total number of boundary and finite elements in the BEM/FEM analysis is 120 and 120, respectively (each horizontal and vertical beam is discretized into 40 and 20 finite elements, respectively). The total number of quadrilateral plate and beam finite elements in the FEM analysis is 800 and 120, respectively. During the optimization, the number of boundary and finite elements is constant, which simplifies significantly the modification of BE and FE discretization. The time of analysis by the Houbolt method is  $600 \mu s$  and the time step  $\Delta t = 2 \mu s$ . The number of chromosomes in the population is 50 and the number of generations of the EA is 100.

### 5.2.1 Dynamic analysis

The accuracy of the developed method is investigated. The analysis is performed for the plate before optimization, called the reference plate, shown in Fig.8 (design

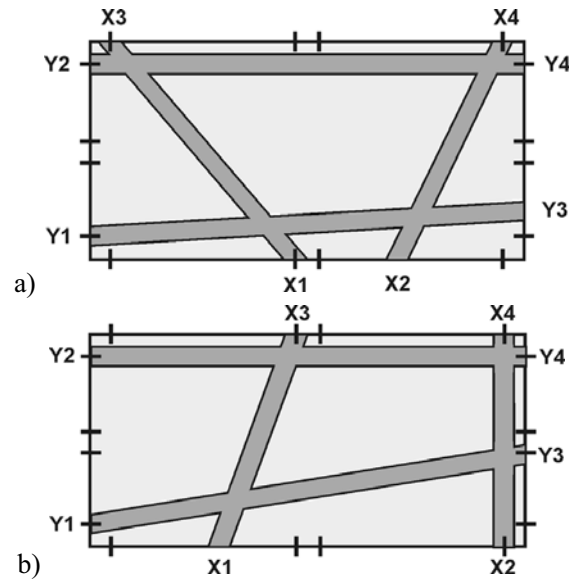


Figure 11 : Optimal structures: a) statics, b) dynamics

variables for this plate are given in Tab.4).

The dynamic vertical displacement at the point A, obtained by the present coupled BEM/FEM and by the professional FEM Nastran code, is presented in Fig.10. As in the previous example of analysis, the agreement of the results is good.

### 5.2.2 Maximization of stiffness

The results of optimization obtained by the evolutionary algorithm, when the criterion of optimization is minimization of the static or maximal dynamic vertical displacement at the point A given by (15), are presented. The values of design variables for the optimal designs, the values of  $J$  and its reduction  $R = (J_o - J) / J_o \cdot 100\%$  (where:  $J_o$  is the  $u^A$  for the plate without stiffeners and  $J$  is the  $u^A$  for the reference or the optimal plate), are shown in Tab.4.

One can observe that the reduction  $R$  for the reference plate and the optimal designs is significant in comparison with the non-stiffened plate.

The optimal structures for statics and dynamics are shown in Fig.11 a and Fig.11 b. It can be seen that in the present example of optimization, most of constraints are active, both for the static and dynamic load.

The dynamic vertical displacement at the point A for the reference, the optimal and the non-stiffened plate is presented in Fig.12. An improvement of dynamic response



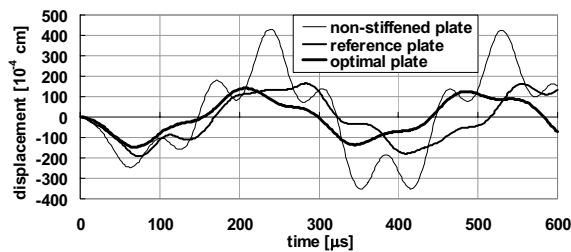


Figure 12 : Displacement at the point A

of the optimal plate in comparison with the non-stiffened and the reference one can be observed.

## 6 Conclusions

In the paper, the formulation and application of the coupled boundary and finite element method to static and dynamic analysis of two-dimensional reinforced structures is presented. The problem of the optimal reinforcement, which gives the highest strength or stiffness, is solved using the evolutionary method. The proposed method requires only discretization of boundaries of the plates and stiffeners. The reduced discretization simplifies modifications of the reinforcement, which is necessary during the optimization process. The results of dynamic analysis are in a very good agreement with the finite element solutions. The evolutionary method can be simply implemented because it needs only the values of objective functions. The probability of obtaining of the global optimal solution is very high, but the method is very time consuming. An improvement of dynamic response is obtained, as the result of optimization, in comparison with the initial design and the structures without reinforcement. The effectiveness of optimization depends on the problem.

## References

- Botta, A.S.; Venturini, W.S.** (2005): Reinforced 2D domain analysis using BEM and regularized BEM/FEM combination. *CMES: Computer Modeling in Engineering & Sciences*, vol. 8, no. 1, pp. 15-28.
- Brebbia, C.A.; Nardini, D.** (1983): Dynamic analysis in solid mechanics by an alternative boundary element procedure. *Soil Dynamics and Earthquake Engineering*, vol. 2, pp. 228-233.
- Coda, H.B.** (2001): Dynamic and static non-linear anal-

ysis of reinforced media: a BEM/FEM coupling approach. *Computers and Structures*, vol. 79, pp. 2751-2765.

**Coda, H.B.; Venturini, W.S.** (1999): On the coupling of 3D BEM and FEM frame model applied to elastodynamic analysis. *International Journal of Solids and Structures*, vol. 36, pp. 4789-4804.

**Coda, H.B.; Venturini, W.S.; Aliabadi, M.H.** (1999): A general 3D BEM/FEM coupling applied to elastodynamic continua/frame structures interaction analysis. *International Journal for Numerical Methods in Engineering*, vol. 46, pp. 695-712.

**Dominguez, J.** (1993): *Boundary elements in dynamics*. Computational Mechanics Publications, Southampton-Boston, Elsevier Applied Science, London-New York.

**Forth, S.C.; Staroselsky, A.** (2005): A hybrid FEM/BEM approach for designing an aircraft engine structural health monitoring. *CMES: Computer Modeling in Engineering & Sciences*, vol. 9, no. 3, pp. 287-298.

**Goldberg, D.E.** (1989): *Genetic algorithms in search, optimization and machine learning*. Addison-Wesley Publishing Company.

**Gorski, R.; Fedelinski, P.** (2004): Optimization of stiffened plates by the coupled BEM/FEM and the evolutionary algorithm, In: *Proceedings of the 6th World Congress on Computational Mechanics in conjunction with the 2nd Asian-Pacific Congress on Computational Mechanics*, Beijing, China, Abstract, Vol. II. Tsinghua University Press, Beijing, Springer-Verlag, Yao ZH, Yuan MW, Zhong WX (eds), pp. 448 (CD-ROM Proceedings - 7 pages).

**Gorski, R.; Fedelinski, P.** (2005): Evolutionary shape optimization of plates with reinforcements, In: *Proceeding of the Third MIT Conference on Computational Fluid and Solid Mechanics*, Cambridge, USA, Elsevier, Amsterdam, The Netherlands, Bathe KJ (ed.), pp. 239-242.

**Leite, L.G.S.; Coda, H.B.; Venturini, W.S.** (2003): Two-dimensional solids reinforced by thin bars using the boundary element method. *Engineering Analysis with Boundary Elements*, vol. 27, pp. 193-201.

**Leite, L.G.S.; Venturini, W.S.** (2005): Boundary element formulation for 2D solids with stiff and soft thin inclusions. *Engineering Analysis with Boundary Elements*, vol. 29, pp. 257-267.

**Michalewicz, Z.** (1996): *Genetic algorithms + data structures = evolution programs*. Springer-Verlag, Berlin.

**Salgado, N.K.** (1998): *Boundary element methods for damage tolerance design of aircraft structures*, Topics in Engineering, Computational Mechanics Publications, Southampton-Boston, vol. 33.

**Salgado, N.K.; Aliabadi, M.H.** (1996): The application of the dual boundary element method to the analysis of cracked stiffened panels. *Engineering Fracture Mechanics*, vol. 54, pp. 91-105.

**Salgado, N.K.; Aliabadi, M.H.** (1999): An object oriented system for damage tolerance design of stiffened panels. *Engineering Analysis with Boundary Elements*, vol. 23, pp. 21-34.

**Zienkiewicz, O.C.; Taylor, R.L.** (2000): *The finite element method. Vol. 1: The basis*. Butterworth-Heinemann, Oxford.